Use of variable sweep for breakdown control was demonstrated for a pitching delta wing. Oscillations of sweep angle with the same frequency as pitching were considered, but with a phase angle. It was shown that, at an optimum phase angle, the amplitude of the variations of breakdown location becomes a minimum. For the optimum phase angle, the amplitude of the swirl angle decreases considerably.

Acknowledgment

This research was supported by U.S. Air Force Office of Scientific Research Grant F49620-92-J-0532.

References

[1]Lee, M., and Ho, C.-M., "Lift Force of Delta Wings," *Applied Mechanics Reviews*, Vol. 43, No. 9, 1990, pp. 209–221.

[2]Rockwell, D., "Three-Dimensional Flow Structure on Delta Wings at High Angle-of-Attack: Experimental Concepts and Issues," AIAA Paper 93-0550, Jan. 1993.

[3]Visbal, M. R., "Computational and Physical Aspects of Vortex Breakdown on Delta Wings," AIAA Paper 95-0585, Jan. 1995.

[4]LeMay, S. P., Batill, S. M., and Nelson, R. C., "Vortex Dynamics on a Pitching Delta Wing," *Journal of Aircraft*, Vol. 27, No. 2, 1990, pp. 131–138.

[5]Gursul, I., and Yang, H., "Vortex Breakdown over a Pitching Delta Wing," *Journal of Fluids and Structures*, Vol. 9, 1995, pp. 571–583.

[6]Hall, M. G., "Vortex Breakdown," *Annual Review of Fluid Mechanics*, Vol. 4, 1972, pp. 195–218.

[7]Gursul, I., Srinivas, S., and Batta, G., "Active Control of Vortex Breakdown over a Delta Wing," *AIAA Journal*, Vol. 33, No. 9, 1995, pp. 1743–1745.

[8]Gursul, I., Yang, H., and Deng, Q., "Control of Vortex Breakdown with Leading-Edge Devices," AIAA Paper 95-0676, Jan. 1995.

[9]Yang, H., "Unsteady Nature of Vortex Breakdown over Delta Wings and Its Control," Ph.D. Thesis, Dept. of Mechanical, Industrial, and Nuclear Engineering, Univ. of Cincinnati, OH, 1996.

[10]Gursul, I., and Ho, C.-M., "Vortex Breakdown over Delta Wings in Unsteady Freestream," *AIAA Journal*, Vol. 32, No. 2, 1994, pp. 433–436.

A. Plotkin
Associate Editor

Approximating Collisional Freestream Attenuation at Transitional Knudsen Numbers

Lyon B. King* and Alec D. Gallimore†
University of Michigan, Ann Arbor, Michigan 48109

Nomenclature

C_1	= arbitrary constant
F	= velocity distribution function
f	= normalized velocity distribution function
I	= total number of scattered molecules
k	= Boltzmann constant 1.38×10^{-23} J/kg K
L	= collision interaction length, m
m	= mass of molecule, kg
n_m	= measured number density, m^{-3}
n_1	= number density of class 1 molecules, m^{-3}
n_2	= number density of class 2 molecules, m^{-3}
n_{1o}	= number density of class 1 molecules at plate surface, m^{-3}
n_{2o}	= number density of class 2 molecules in freestream, m^{-3}
q	= dynamic pressure, Pa
T_p	= plate surface temperature, K
u_o	= bulk velocity of freestream, m/s
v_n	= velocity normal to plate surface, m/s
x	= streamwise position coordinate, m
δ	= Dirac function
κ	= pressure amplitude constant [Eq. (13)]
λ	= mean free path, m
σ_{12}	= total collision cross section, m^2
$\Phi_i^{(x)}$	= incident flux of quantity x
$\Phi_r^{(x)}$	= reflected flux of quantity x

Received April 2, 1996; revision received Oct. 17, 1996; accepted for publication Nov. 6, 1996; also published in *AIAA Journal on Disc*, Volume 2, Number 2.

*Graduate Student Researcher, Plasmadynamics and Electric Propulsion Laboratory, Department of Aerospace Engineering. Student Member AIAA.

†Assistant Professor, Plasmadynamics and Electric Propulsion Laboratory, Department of Aerospace Engineering. Member AIAA.

Introduction

WHEN a body such as an instrument package is immersed within a rarefied flowfield, the inevitable result is distortion of the freestream. This perturbation is a formidable stumbling block for code developers seeking reliable experimental data for comparison with flowfield predictors. A special interest of late has been the determination of the true freestream dynamic pressure for an exoatmospheric plume. This effort has been inspired by the desire to create an accurate plume flowfield predictor for the Space Shuttle Orbiter's primary reaction control thrusters.[1] Current codes produce a spatial map of dynamic pressure. Validation of the codes must rely on an accurate means of determining the undisturbed freestream dynamic pressure from experimental data for comparison. Although this problem is closed for a continuum case via the Rayleigh–Pitot formula, the extreme low density inherent to an exoatmospheric plume renders this treatment invalid because the thickness of the shock layer may be many times larger than the body immersed in the flow.

Analytical Model

The basic approach taken to solve this problem was to analyze the interaction between two separate streams of molecules. Molecule class 2 represents the undisturbed freestream of the thruster plume; molecule class 1 represents the molecules that previously have impacted the plate and have been reflected from its surface. The positive x direction is taken toward the plate, parallel with the freestream velocity. The location of $x = 0$ corresponds with the outermost edge of the defined collision zone, with $x = L$ coincident with the plate surface. The assumptions utilized in the model are presented here a priori and will be referenced throughout the solution.

1) *The directed bulk flow velocity is high in comparison with the random thermal velocity within the freestream molecules (very large speed ratio).* A Dirac probability density function will preselect molecules with this limiting velocity while not allowing molecules with any other speeds: $F_2 = n_2\delta(v_z)\delta(v_y)\delta(v_x + u_0)$.

2) *Molecules impacting the plate are fully accommodated and reemitted in thermal equilibrium with the plate (diffuse reflection).* The result of this assumption is that molecules reflected from the plate will have a half-Maxwellian distribution, F_1, at temperature T_p and density n_{1o}.

3) *The velocity of class 2 molecules is much greater than that of class 1 molecules.* This assumption requires the velocity of the freestream molecules to be much greater than the thermal speed of the Maxwellian plate molecules. Utilizing assumption 1, this requires $u_0 \gg (kT_p/\pi m)^{1/2}$.

The remaining assumptions (presented below) pertain to the intermolecular collision phenomena of the transitional flow regime. In this regime the theory takes on the form of a First-Collision Theory, accounting for some molecular collisions while neglecting other collisions. In this First-Collision treatment of the problem, the following assumptions were made:

4) *Intermolecular collisions are characterized by hard-sphere interactions.*

5) *Class 1 molecules are collisionless with respect to other class 1 molecules. Similarly, class 2 molecules are collisionless with respect to other class 2 molecules. The only collisions of significance are those arising between class 1 and class 2 molecules.*

6) *Any collision between a class 1 and a class 2 molecule causes both molecules to be scattered such that neither molecule intersects with the plate surface. In addition, these scattered molecules do not*

undergo any collisions with other class 1 or class 2 molecules prior to escaping from the analyzed volume.

7) *The intermolecular collisions occur within a defined shock layer in front of the plate ranging from the plate surface to a distance L in front of the plate.*

The first step in solving this problem is to analyze the effect of intermolecular collisions between the two streams of molecules. The total number of molecules scattered by collisions at position x is given by

$$I(x) = \tfrac{1}{2}\sigma_{12} u_o n_1(x) n_2(x) \tag{1}$$

Using the concept of mean free path,[2] one can calculate the decay of the number densities due to collisions. The fraction of class 2 molecules that survives a distance x without undergoing a scattering collision is given by the well-known survival equation

$$\frac{n_2(x)}{n_{2o}} = e^{-(x/\lambda)} \tag{2}$$

A similar expression can be written for class 1 molecules with a simple coordinate transformation, with the result that

$$\frac{n_1(x)}{n_{1o}} = e^{(x-L)/\lambda} \tag{3}$$

where L is the distance in front of the plate over which intermolecular collisions occur. The total number of molecules that undergo a scattering collision during the interaction now can be integrated from Eq. (1) because we know the number densities as a function of x:

$$\begin{aligned} I_{\text{scat}} &= \frac{1}{2}\sigma_{12} u_o \int_0^L n_1(x) n_2(x)\,\mathrm{d}x \\ &= \frac{1}{2}\sigma_{12} u_o n_{1o} n_{2o} L e^{-(L/\lambda)} \end{aligned} \tag{4}$$

We now have a closed-form relation for the total flux of scattered molecules over a finite interaction length L. Note in the preceding integral that the mean free path λ was assumed to be constant. In reality, because the number densities change with x, the mean free path also will be a function of x. However, as a first-order analysis, the mean free path is approximated as constant and equal to the mean free path between the undisturbed freestream and the undisturbed reflected molecule flux.

Now that we know the total flux of scattered molecules from Eq. (4), we can employ assumption 6: All scattering collisions will cause both molecules to miss the plate and hence be removed from our analysis. The total flux of molecules that reaches the plate surface is then the difference between the freestream flux and the scattered flux: $I_{\text{meas}} = I_{2o} - I_{\text{scat}}$. The freestream molecule flux takes on a simple form because of our assumption of a Dirac probability density function, namely $I_{2o} = n_{2o} u_o$. So the measured flux becomes

$$I_{\text{meas}} = n_{2o} u_o \left[1 - \tfrac{1}{2}\sigma_{12} n_{1o} L e^{-(L/\lambda)}\right] \tag{5}$$

Because of assumption 6, the only molecules reaching the plate surface will be those class 2 (freestream) molecules that have not undergone a collision. Because these molecules have not collided with other molecules, their probability density function will remain the unaltered freestream Dirac function. So the flux of molecules reaching the plate, I_{meas}, is simply $n_m u_o$. We now have the condition that

$$n_m = n_{2o}\left[1 - \tfrac{1}{2}\sigma_{12} n_{1o} L e^{-(L/\lambda)}\right] \tag{6}$$

where the mean free path λ is given by

$$\lambda = \frac{1}{\sigma_{12} n_{1o}} \tag{7}$$

Utilizing this definition of λ and rearranging Eq. (6), we obtain

$$n_m / n_{2o} = 1 - (1/2\lambda) L e^{-(L/\lambda)} \tag{8}$$

Equation (8) gives the ratio between the number density reaching the surface and freestream density. The only problem with closing the equation is the unknown quantity n_{1o}, the number density of particles leaving the plate surface, which is required to specify λ. However, a relation can be derived for n_{1o} by considering the mass flux at the plate surface.

The mass flux incident to the plate surface again has a simple form owing to the Dirac distribution function of the particles reaching the plate, $\Phi_i^{(m)} = m n_m u_0$. The mass flux reflected from the plate is slightly more complicated but can still be evaluated analytically because of our assumption of full accommodation:

$$\Phi_r^{(m)} = m n_{1o} \sqrt{kT_p / 2\pi m} \tag{9}$$

Under equilibrium conditions it is safe to assume that the incident mass flux is equal to the reflected mass flux. Utilizing this relation gives us a closed form for n_{1o}:

$$n_{1o} = n_m u_o \sqrt{2\pi m / kT_p} \tag{10}$$

We now have a closed expression for the ratio between the measured and freestream number densities as a function of known quantities by substituting Eq. (10) into Eq. (8):

$$n_m / n_{2o} = 1 - \tfrac{1}{2}\sigma_{12} n_m u_o \sqrt{(2\pi m / kT_p)}\, L e^{-L\sigma_{12} n_m u_o \sqrt{2\pi m / kT_p}} \tag{11}$$

A more interesting quantity to look at is how this reduction in freestream particle flux affects the pressure imparted to the plate surface. The pressure at the plate is not entirely specified by the incident momentum flux $m n_m u_o^2$. Because of our assumption of full accommodation, there is a second component of momentum induced by the reemission of the molecules: The molecules impart momentum to the plate when they hit and stick to the surface, then impart more momentum when they are reemitted from the plate with a half-Maxwellian distribution. The pressure on the plate is the sum of these two momentum fluxes. The flux of incident normal momentum is given by $\Phi_i^{(mv_n)} = m n_m u_o^2$. The reflected component of normal momentum flux is a bit more complicated by the Maxwellian distribution of the reemitted molecules, but it still can be integrated analytically:

$$\Phi_r^{(mv_a)} = \tfrac{1}{2} n_{1o} k T_p \tag{12}$$

The reflected momentum flux involves the reflected number density n_{1o}; however, we derived an expression for this quantity as a function of n_m when we required the net mass flux at the plate to be zero [Eq. (10)]. Utilizing this relation,

$$\Phi_r^{(mv_n)} = \tfrac{1}{2} n_m u_o \sqrt{2\pi m k T_p} \tag{13}$$

The pressure measured at the plate surface is the sum of incident and reflected momentum fluxes

$$P_m = m n_m u_o^2 + \tfrac{1}{2} n_m u_o \sqrt{2\pi m k T_p} \tag{14}$$

Equation (14) can be solved for n_m as a function of measured pressure P_m. Substituting this expression into Eq. (11) and recognizing that $m n_{2o} u_o^2$ is equal to twice the freestream dynamic pressure q_∞ yields

$$\begin{aligned} \frac{P_m}{2q_\infty} = \frac{1}{\kappa}\Bigg\{1 - \frac{P_m}{2}\left(\frac{L\sigma_{12}}{2mu_o + \sqrt{2\pi m k T_p}}\sqrt{\frac{2\pi m}{kT_p}}\right) \\ \times \exp\left[-\left(P_m \frac{L\sigma_{12}}{2mu_o + \sqrt{2\pi m k T_p}}\sqrt{\frac{2\pi m}{kT_p}}\right)\right]\Bigg\} \end{aligned} \tag{15}$$

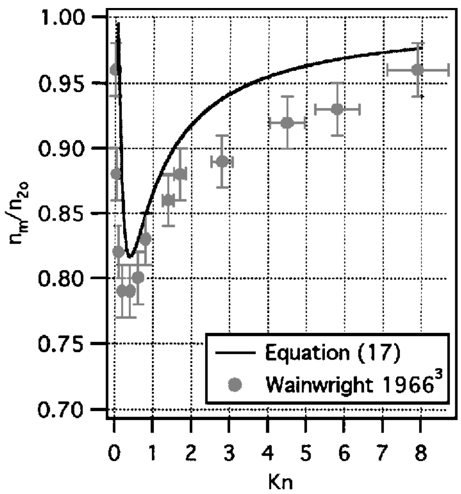

Fig. 1 Comparison of front face scattering data from Wainwright and Rogers[3] with Eq. (17) for a constant $C_1 = 0.4$ (error bars added to reflect uncertainty in reading data from original paper).

where the constant κ is defined as

$$\kappa \equiv \frac{m u_o^2}{m u_o^2 + \frac{1}{2} u_o \sqrt{2\pi m k T_p}} \tag{16}$$

Discussion

The model as presented has some intriguing qualities. If we assume that the depth of the collision sheath scales with a physical length scale in the flow so that $L/\lambda = Kn^{-1}$, Eq. (17) can be compared directly with data obtained by Wainwright and Roger.[3] Because the parameter L was only loosely defined, we are free to insert a constant C_1 in front of it as a free parameter and should expect the value of the constant to be on the order of unity:

$$n_m/n_{2o} = 1 - \tfrac{1}{2}(C_1 L/\lambda)e^{-(C_1 L/\lambda)} \tag{17}$$

Wainwright and Roger used impact probes of varying size and with different probe face geometries to quantify the effect of molecular scattering at transitional Knudsen numbers. Figure 1 compares Wainwright's data with Eq. (17) for a value of $C_1 = 0.4$, with L equal to the diameter of the impact probe face. The agreement between Eq. (17) and the data is excellent. The relative difference between the two is less than 4%. The largest effect of intermolecular collisions occurs expectedly in the regime of $0.5 < Kn < 1$. As the Knudsen number further increases, and the flow approaches free molecular, the ratio of measured density to freestream density tends toward unity. This is expected because the molecules will no longer scatter at such large relative mean free paths and the incident and reflected streams will move through each other unperturbed.

Acknowledgments

This work was sponsored by the NASA Johnson Space Center (JSC) under Contract NAG9-709. This support is gratefully acknowledged. The authors would like to thank Ricardo Machin of JSC (Contract Monitor) for his assistance and advice, as well as Steve Fitzgerald.

References

[1]Fitzgerald, S. M., Rocha, R. A., Bouslog, S. A., Hughes, J. R., and Leahy, K. S., "Far Field Plume Characterization Testing in Support of Space Station Plume Impingement Methodology Validation," AIAA Paper 94-2636, June 1993.

[2]Gombosi, T. I., *Gaskinetic Theory*, Cambridge Univ. Press, Cambridge, England, UK, 1994.

[3]Wainwright, J. B., and Roger, K. W., "Impact Pressure Probe Response Characteristics in High Speed Flows with Transition Knudsen Numbers," *Proceedings of 4th International Symposium on Rarefied Gas Dynamics*, edited by J. H. deLeeuw, Vol. 2, 1966, pp. 151–174.

G. Laufer
Associate Editor

Attenuation of Shock Waves in Gas-Particle Mixtures

H. K. Das* and J. Kurian†
Indian Institute of Technology, Madras 600036, India

Introduction

SHOCK waves formed within a gas-particle mixture have characteristics different from the pure gas case. Decay of the shock wave has been studied by a number of researchers applying different numerical methods. Compared with theoretical investigations, only a few experimental works are reported on the study of shock wave attenuation. Sommerfeld and Gronig,[1] Sommerfeld,[2] and Igra et al.[3] conducted experiments on a vertical shock tube along with numerical calculation. Olim et al.[4] and Aizik et al.[5] compared their numerical results with the experimental results of Sommerfeld.[2] The purpose of the present Note is to add more experimental results on decay process of shock waves in gas-particle mixtures inside a shock tube.

Details of Experiments

The experiments were conducted with a stainless steel horizontal shock tube 50 mm in diameter and 6 m long. The driven section is 4.5 m long and the diaphragms used were of aluminum foil. Diaphragms of different thicknesses from 0.05 to 0.25 mm were used. Rupture of a diaphragm was accomplished with high pressure on the driver side. A particle injection system was designed to produce a uniform flow rate of particles fed into the driven section immediately downstream of the diaphragm before each shock tube run. The injection system consisted of an inlet system, a particle reservoir, a convergent-divergent(CD) nozzle, a mixing chamber, and an exhaust system. The exit of the particle reservoir was placed in the diverging portion of the CD nozzle, causing particles to get sucked in by the low pressure created in the airstream when a sufficiently high-pressure air was fed into the inlet system. Particles were mixed with air in the mixing chamber and the gas-particle mixture was fed to the shock tube immediately after the diaphragm. The particles used in the experiments were Ballotini spheriglass and precipitated calcium carbonate powder. Particle material densities were 2500 and 2790 kg/m^3, respectively. Both types of particles had size distributions and average particle sizes were determined using a Malvern laser diffraction particle sizer. Mean diameter for calcium carbonate powder was 6.9 μm and that of glass particles was 34.4 μm. Photomicrographs of the particles showed the shape of the particles to be very nearly spherical.

Laser Light Extinction Technique

A beam of light from a continuous wave, He-Ne laser is made to transverse the shock-tube test section and to fall on a photodetector. The intensity of the laser beam was measured before the start of the gas-particle injection as I_0. With the gas-particle flow in the test section, the intensity is reduced to I, which is related to the initial intensity by the Lambert–Beer equation as

$$I/I_0 = \exp(-k\rho_p) \tag{1}$$

where k is a constant that includes the extinction coefficient and ρ_p is the cloud density. In the present experiments, a pin photodiode (PIN SPOT 8D, United Detector Technology) is employed as a photodetector. The output voltage E of the photodiode is directly proportional to the intensity of light incident on it. Hence, the expression of Beer's law can be written as the ratio of the voltage

Received April 30, 1996; revision received Oct. 1, 1996; accepted for publication Oct. 8, 1996; also published in *AIAA Journal on Disc*, Volume 2, Number 2.

*Research Scholar, Department of Aerospace Engineering.
†Associate Professor, Department of Aerospace Engineering.